Extensive gaseous haloes surrounding giant elliptical galaxies - Evidence from depolarization in radio galaxies

Strom, R.G.; Jaegers, W.J.

Astron. Astrophys. 194, 79–89 (1988)

ASTRONOMY
AND
ASTROPHYSICS

Extensive gaseous haloes surrounding giant elliptical galaxies: evidence from depolarization in radio galaxies

R.G. Strom [1] **and W.J. Jägers** [2]

[1] Netherlands Foundation for Radio Astronomy, Postbus 2, 7990 AA Dwingeloo, The Netherlands
[2] Sterrewacht, Postbus 9513, 2300 RA Leiden, The Netherlands

Received July 6, accepted October 8, 1987

Summary. Radio polarization measurements have been used to investigate large scale gaseous components associated with some thirteen double radio sources. At 49 cm a significant proportion of the bridge emission, roughly centered on the parent galaxy, is invariably found to be unpolarized. We present evidence that this lack of polarization at long wavelengths is the result of differential Faraday rotation in a large scale halo associated with the central (usually elliptical) galaxy. The haloes, which extend beyond 100 kpc, appear to be the outer envelopes of hot gas such as that observed in the form of extended X-ray emission associated with a number of nearby early-type galaxies. The depolarization observed in the two largest sources indicates decreasing gas density with increasing radius, with a typical value of $3\ 10^{-5}\,\mathrm{cm}^{-3}$ at 100 kpc. Combining radio and X-ray density estimates, we find that the behavior is consistent with gas in hydrostatic equilibrium trapped in the gravitational potential well of a central galaxy. The data imply total masses for these galaxies of several times $10^{12}\,M_{\odot}$, while the mass detected in the haloes is but a fraction of this. Only for radii exceeding 1 Mpc would the halo mass approach that of a giant elliptical galaxy. There is no evidence for substantial amounts of additional ("dark") matter mixed in with the gas detected by depolarization. The surface densities implied ($4\ 10^{19}\,\mathrm{cm}^{-2}$ at a radius of 200 kpc for $z \approx 0.1$) are not unlike those found in the Lyα forest of absorption features in distant quasars, although other facts suggest that the two phenomena may not be related.

Key words: coronae of elliptical galaxies – polarization – Faraday effect

1. Introduction

The effects of differential Faraday rotation upon the polarization of radio sources have been well-understood for about twenty years (Burn, 1966; Gardner and Whiteoak, 1966). The degree of linear polarization will, on average, decrease with increasing wavelength, both in localized regions of emission and for the source taken as a whole. Conway et al. (1972) found that the median degree of polarization of extragalactic source samples decreases at long wavelengths such as 49 and 73 cm. Indeed, on average, the degree of polarization at wavelengths of 30 cm and longer would appear to be a fair diagnostic for depolarization by differential Faraday rotation, and was used as such, for example, in studies by Strom (1973a), and Conway and Gilbert (1970).

The primary reason for depolarization is an excess in the amount of Faraday rotation in some polarized regions when compared with others (Burn, 1966). Strom (1973a) suggested that depolarization was largely intrinsic, related to the source linear size. Moreover, he found that sources of larger angular diameter showed less depolarization than the compact ones, suggesting that the effects of depolarization in a screen far from the source (in the Galaxy, for example) were probably negligible. This seems to be confirmed by studies of very large radio galaxies (Willis and Strom, 1978; Strom and Willis, 1980; Willis et al., 1981) which all have high degrees of polarization at 49 cm and show little evidence for differential Faraday rotation.

Intrinsic (i.e., source-related) causes of depolarization of various types have been suggested in the past. Strom (1973b) pointed out that a correlation with source size could explain the excess depolarization of high redshift objects, there being a deficiency of intrinsically large radio sources at large redshifts in the samples studied. Conway et al. (1974), on the other hand, suggested that the primary correlation was between depolarization and source luminosity. Recently, Strom and Conway (1985), extending a study made by Conway et al. (1983), found evidence in 49 cm maps for excess depolarization in source bridges, and suggested that the effect was related to ionized gas associated with the optical parent object (galaxy or quasar). The purpose of this paper is to examine the effect further, using additional data obtained by Jägers (1987) with the Westerbork Synthesis Radio Telescope (WSRT).

2. Observational data

Part of the weakness of Strom and Conway's (1985) analysis was that it largely depended upon 49 cm maps of some eight sources. Recently, Jägers (1987) has completed a study of very extended northern hemisphere radio sources at 49 and 21 cm. This data set provides us with additional sources, higher quality maps, and in particular a second, shorter wavelength, to be able to test whether we are indeed seeing the effects of differential Faraday rotation. Details of the observation and data reduction can be found in Strom and Conway (1985) and Jägers (1987). The sources and data sets available are summarized in Table 1. Only one source, 3C 223, is common to both sets of data. A comparison of its 49 cm

Table 1. Sources included in the study

Name	Data available (wavelength, in cm)	Ref.[a]
3C 33.1	21, 49	J 87
3C 35	21, 49	J 87
3C 79	49	SC 85
3C 111	21, 49	J 87
B 0844+316	21, 49	J 87
3C 223	21, 49	J 87, SC 85
3C 223.1	49	SC 85
3C 234	49	SC 85
3C 265	49	SC 85
3C 274.1	49	SC 85
3C 284	49	SC 85
3C 390.3	21, 49	J 87
3C 452	21, 49	J 87

[a] J 87 – Jägers (1987); SC 85 – Strom and Conway (1985)

maps shows excellent agreement, both in the total intensity and polarized distributions, despite the fact that Strom and Conway (1985) obtained sparser coverage of the visibility plane.

In addition to the corrections specified in the original articles, an additional effect must be taken into account, especially at 21 cm. This is the contribution of the central nuclear source (if visible) to the bridge emission. Since we are only interested in the polarization of the extended bridge component, it would be wrong if our integrations included the compact nucleus. Only three sources are affected: 3C 35, 3C 111, and 3C 390.3. None of the nuclear components appears to be significantly polarized, a trend which is confirmed by recent observations of a sample of such objects (Rudnick et al., 1986). The correction therefore consisted of estimating the component flux and removing it from the source brightness distribution. This was done wherever we have determined the degree of polarization, and will be so noted in the text.

3. Results

The data have been analyzed in two ways. To compare all data sets with sufficient signal to noise, we have performed integrations of the total intensity and polarization distributions over the relevant constituent source parts, components and bridges. Because some components display position angle changes on opposite sides which might result in apparent depolarization when there is none, the integration was performed on maps of $P(=[Q^2+U^2]^{1/2})$. For three sources which are well-resolved, we have also analyzed the polarization distribution along the source major axis, in an attempt to see how depolarization varies with position.

A statistical indication of the source depolarization is given in a series of histograms. We have integrated the source emission over regions of about 120 kpc in size, centered on the optical object, and each of the outer hot spots. Figure 1 shows the 49 cm degree of polarization for (a) bridges and (b) the components. It is clear that the same trend is present in both sets of objects: components are more strongly polarized at 49 cm than bridges.

In Fig. 2 we show the degree of polarization determined in precisely the same way at 21 cm for the sources studies by Jägers (1987). Although the median degree of polarization of bridges is a bit lower than that of the components, the difference is far less striking than at 49 cm and for one bridge component the polarization is very high at 21 cm. The lower degree of polarization for the bridge emission may be intrinsic, although it could also indicate that even at 21 cm some depolarization is present.

Figure 3 shows that the effect is most likely related to Faraday depolarization. The depolarization parameter, D_{21}^{49} (= % polarization at 49 cm/% polarization at 21 cm; so defined, D is small when there is much depolarization), is substantially lower for the bridges than the components.

To investigate the general trend over the entire distance spanned by the source components further, we have determined D_{21}^{49} for the sources observed by Jägers (1987) at intervals along each component axis of slightly less than one synthesized beamwidth. The values have been grouped according to their distance from the optical galaxy. Data points where the 21 cm degree of polarization is $\leqq 5\%$ have not been included. The average value of D_{21}^{49} for each bin is shown as a function of median bin distance in Fig. 4. We have tested the data by means of a least squares fit and find that D increases with increasing distance from the optical galaxy (dashed line), producing a coefficient of determination of 0.85.

Let us now turn to several individual cases. We will discuss the distributions in 3C 33.1, 3C 35, and 3C 223 in turn.

3C 33.1

The distributed linear polarization ($P=[Q^2+U^2]^{1/2}$) and degree of polarization ($\% = 100\,P/I$) at both 21 cm and 49 cm from Jägers (1987) are reproduced in Fig. 5. By intercomparing these four maps one obtains a fair impression of how depolarization

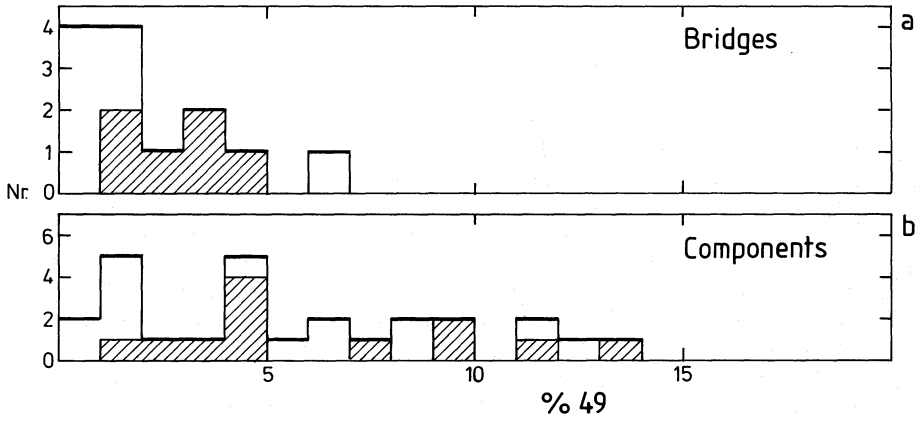

Fig. 1a and b. Histograms of the integrated degree of polarization at 49 cm for **a** bridge emission centered on the optical galaxy and **b** the outer components near the hot spots. Crosshatching indicates the sample studied by Strom and Conway (1985)

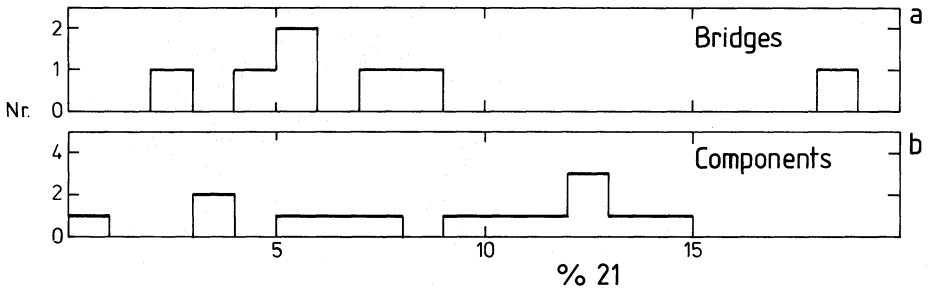

Fig. 2a and b. Histograms of the integrated degree of polarization at 21 cm for **a** bridge emission and **b** outer components

proceeds throughout the source, something which is less clear in a map of D_{21}^{49} (Jägers, 1987). Because of the eccentric location of the optical galaxy, depolarization appears to extend well into the northeastern lobe at 49 cm. Even at 21 cm there may be excess depolarization in this region, underlining the need for additional studies at even shorter wavelengths. [6 cm polarization observations (Van Breugel and Jägers, 1982) show values up to 65% and suggest that there probably is depolarization at 21 cm.] Because of these complications, the picture which emerges from crosscuts through the source (Fig. 6) is not so clear-cut. The depolarization ratio (Fig. 6b) reaches its lowest value northeast of the optical galaxy, but the higher value of D_{21}^{49} in the galaxy's immediate vicinity (where, in fact, we only have an upper limit) may be partly because of the low degree of polarization at both 21 and 49 cm there.

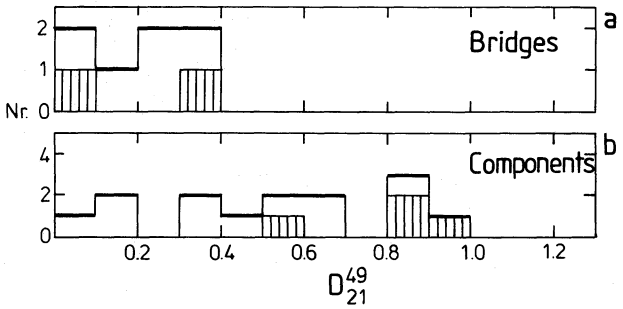

Fig. 3a and b. Histograms of the ratio of the degree of polarization at 49 cm to that at 21 cm, D_{21}^{49}, for **a** source bridges and **b** outer components. Crosshatching indicates the values for the two sources of greatest overall linear size

3C 35

The maps (Fig. 7) clearly show the dramatic disappearance of polarization from the bridge region in going from 21 to 49 cm. Note in particular that the optical galaxy is left in a bay of low polarization at 49 cm. In the crosscuts (from which the effects of the nuclear component have been removed), Fig. 8, the dip in D_{21}^{49} clearly lies close to the position of the galaxy. Note also, however, that in the components themselves there are several other drops in D_{21}^{49} associated with local depolarization.

3C 223

This source offers the most clear-cut case of depolarization. The maps (Fig. 9) illustrate the sudden disappearance of polarization from the vicinity of the galaxy at 49 cm. The degree of polarization found at 6 cm (Van Breugel and Jägers, 1982) in those regions where it could be detected is similar to that at 21 cm, confirming the depolarization interpretation. In the crosscut we see how only the 100 kpc region surrounding the galaxy has $D_{21}^{49} < 0.5$, clearly demonstrating the presence of excess Faraday depolarization (Fig. 10).

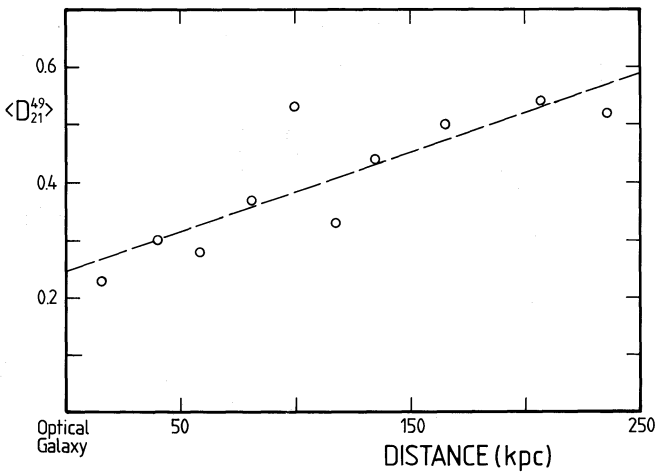

Fig. 4. Average values of D_{21}^{49} as a function of distance from the optical galaxy for the sources studied by Jägers (1987). The bin width (along the abscissa) has been determined by the requirement that an equal number of measurements should go into each average. The dashed line is a least squares fit to the data points

4. Discussion

Despite certain ambiguities, which is hardly surprising since there are probably several competing effects contributing to excess magneto-ionic material, and hence depolarization, in extragalactic radio sources, we suggest that there is evidence for material associated with the optical parent object (in our case, always an elliptical galaxy) in these radio galaxies. The most obvious candidate is a halo of gas, and we will now consider what its properties as defined by these radio observations are, beginning with an estimate of typical densities.

The size over which the effect is especially noticeable is about 100 kpc [1] as can be seen from both the statistical depolarization trend (Fig. 4) and that of the individual sources (Figs. 6, 8 and 10). The depolarization occurs between 21 and 49 cm so we will adopt $\lambda_{1/2} = 30$ cm (see Strom, 1973a). A typical value for the line of sight magnetic field strength (estimated as outlined under Eq. (2) below) in the bridge region is 2 μG, and combined with the other

[1] Assuming $H_0 = 50\,\mathrm{km\,s^{-1}\,Mpc^{-1}}$

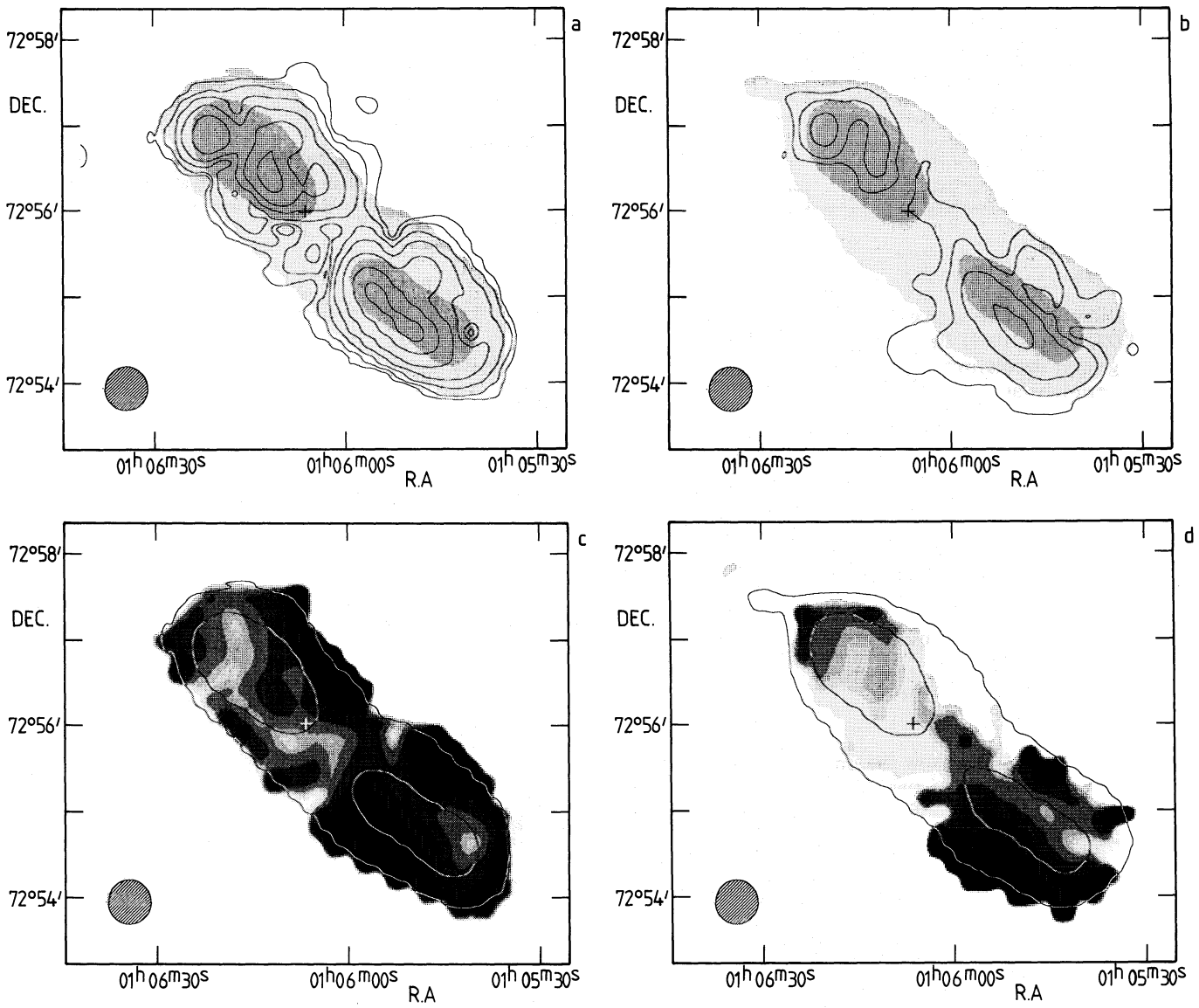

Fig. 5a–d. The polarization distribution in 3C 33.1. The polarized intensity P is shown as contours superimposed upon the total intensity brightness distribution I in gray at **a** 21 cm (contour values: 0.75, 1.5, 3, 6, 12, 24, and 36 mJy beam^{-1}) and at **b** 49 cm (contour values: 5, 10, 20, and 40 mJy beam^{-1}). The degree of polarization is shown as gray shading with contours from the total intensity at **c** 21 cm and **d** 49 cm. The lightest shade of gray indicates a value below 2%. Thereafter, the degree of polarization increases logarithmically to 20% (black). A cross indicates the position of the optical galaxy

values this gives an electron density, $n_e \simeq 10^{-4}\,\mathrm{cm}^{-3}$. If this uniformly fills the entire volume, then it suggests a mass of $2\ 10^9\ M_\odot$. (A higher mass results if the density is enhanced near the galaxy, which is probably the case as we will see below.)

There have been several reports in recent years of X-ray emission from extensive, hot haloes surrounding large (but not in general radio emitting) early-type galaxies (e.g., Biermann and Kronberg, 1983; Nulsen et al., 1984; Forman et al., 1985, and references therein). These suggest that a hot halo component is fairly common among giant ellipticals, and the typical densities derived are 10^{-2} to $10^{-3}\,\mathrm{cm}^{-3}$ in a diameter of typically 10 to 20 kpc. Biermann and Kronberg point out that this component may extend to greater distances with a density too low for the X-ray emission to be detectable, just as the radio polarization indicates.

While it might seem logical to look for such emission in radio galaxies, this is problematical on several counts. Radio galaxies are generally too distant for the emission expected from a hot component to have been detected with EINSTEIN or similar telescopes. Moreover at such distances it would be difficult to resolve a 10 kpc object, so one would not be absolutely certain whether the emission, if detected, is diffuse (all the galaxies studied are thus quite nearby). And finally, radio galaxies, which are active objects, often show X-ray nuclear emission, confusing the issue (e.g. Feigelson et al., 1984; Miller et al., 1985, who detect unresolved X-ray emission from 3C 223 at a luminosity more than ten times greater than that of the thermal emission measured in other sources). Forman et al. (1985) have, nevertheless, unambiguously demonstrated the presence of extended X-ray emission around several active galaxies including some with radio emission.

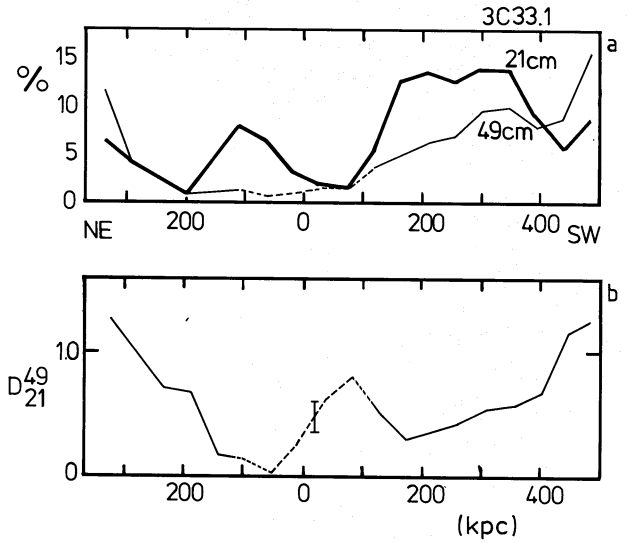

Fig. 6a and b. Cross cuts along the major axis of 3C 33.1 for **a** the degree of polarization at the two wavelengths and **b** the depolarization ratio D_{21}^{49}. Dashed lines indicate upper limits to the values, and an error bar gives the typical uncertainty in a region where it is much greater than the line thickness

The densities implied by the X-ray components are so large they will produce depolarization at wavelengths of 6 cm or less. However, that will all happen well within the beam used in the present study, so the effect will essentially be washed out by beam dilution. We will now investigate whether there is continuity between the densities derived from the X-ray and radio data, and what this implies about the structure of the gaseous haloes.

The X-ray flux density, S, depends upon the density of thermal plasma, n_{th}, for a fixed gas temperature as

$$S \propto \int n_{th}^2 \, dl, \tag{1}$$

where l is the distance along the line of sight. Consequently, the X-ray observations can be used to estimate n_{th} for an assumed temperature. Forman et al. (1985) have analyzed X-ray measurements of hot haloes around early-type galaxies and have extracted physical parameters for some 13 objects. The observations were carried out using the imaging instruments (IPC and HRI) aboard the Einstein Observatory. In a further analysis which included the same data, Thomas et al. (1986) have extracted radial profiles of various physical quantities for a number of galaxies. Both of these investigations show that the densities, masses and their variations with radius are quite similar.

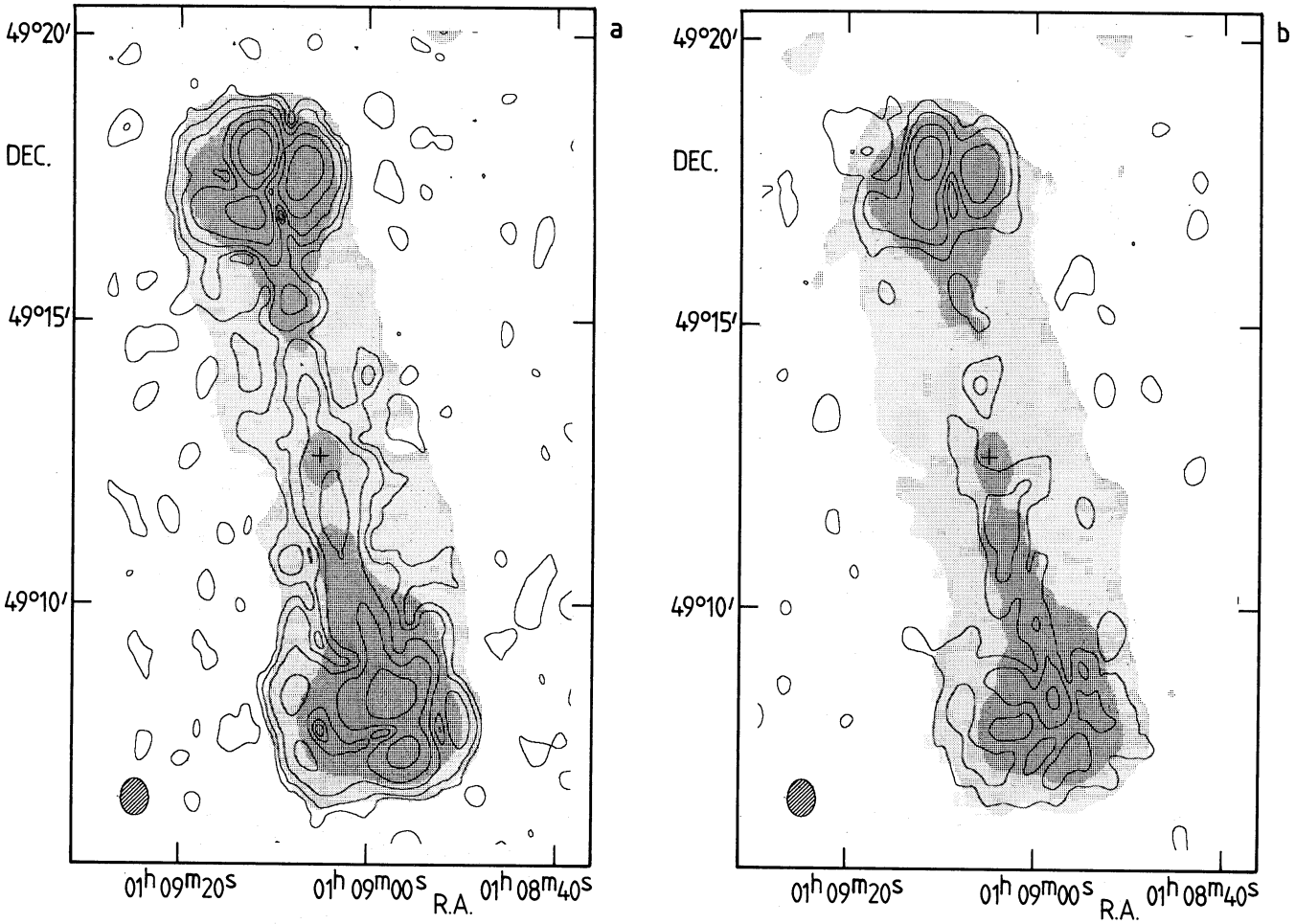

Fig. 7a–d. The polarization distribution in 3C 35. The polarized intensity P is shown as contours superimposed upon the total intensity brightness distribution I in gray at **a** 21 cm (contour values: 0.5, 1, 2, 4, 8, and 16 mJy beam^{-1}) and at **b** 49 cm (contour values: 3, 6, 12, and 24 mJy beam^{-1}). The degree of polarization is shown as gray shading with contours from the total intensity at **c** 21 cm and **d** 49 cm. The lightest shade of gray indicates a value below 2%. Thereafter, the degree of polarization increases logarithmically to 20% (black). A cross indicates the position of the optical galaxy

For twelve galaxies, Forman et al. (1985) have fitted the observed X-ray surface brightness distributions as a function of radius, r, to profiles of the form $[1+(r/r_c)^2]^{-3\beta+1/2}$ to determine β and the core radius, r_c. The values of β cluster around, and are all consistent with, 0.5, while r_c ranges from about 1 to 9 kpc. Consequently, when $r=r_c$ the surface brightness has fallen to about half is peak value. We have used the density profiles obtained by Thomas et al. (1986) to estimate n_{th} at r_c for twelve early-type galaxies. In addition, improved values for NGC 5846 (Biermann and Kronberg, 1983) have been provided by Biermann (private communication). For NGC 3607 (Biermann et al., 1982) the parameters have been estimated by comparison with NGC 1395 (Nulsen et al., 1984) which is similar in most respects. A list of the galaxies, their types (De Vaucouleurs et al., 1976), r_c and n_{th} appears in Table 2. We note that the nearby radio galaxy NGC 5128 (Cen A), in which the halo emission is confused by other X-ray components, appears to be quite similar to the galaxies in Table 2: Feigelson et al. (1981) find a density of $3\ 10^{-3}\,\mathrm{cm}^{-3}$ at 5.4 kpc from the nucleus. The values in Table 2 will be used for our comparison with particle densities derived from the radio polarization measurements.

For the Faraday depth, Φ, we have:

$$\Phi \propto \int n_e B_{\|}\, dl\,. \tag{2}$$

We have analyzed the polarization data in the central bridge regions of the two largest radio galaxies in our sample, 3C 35 and 3C 223. First, assuming that the emission is cylindrically symmetric about the source major axis, the line of sight depth through each source has been determined at intervals of slightly less than one-half the beamwidth along the major axis. The average volume emissivity has been used to determine the equipartition magnetic field strength which, combined with the degree of polarization at short wavelengths and making the usual assumptions (Burn, 1966), enables us to estimate the strength of the uniform component of the magnetic field. Using the values for D_{21}^{49} (Figs. 8 and 10), the magnetic field strength and line of sight depth together with the relationship in Eq. (2), we have determined n_e over distances ranging from about 40 to 230 kpc from the nuclei (the calculation was halted where D_{21}^{49} approaches 1 or begins to decrease). Assuming $n_e \simeq n_{th}$, we can then compare the densities *from different sources* derived from X-ray and radio data.

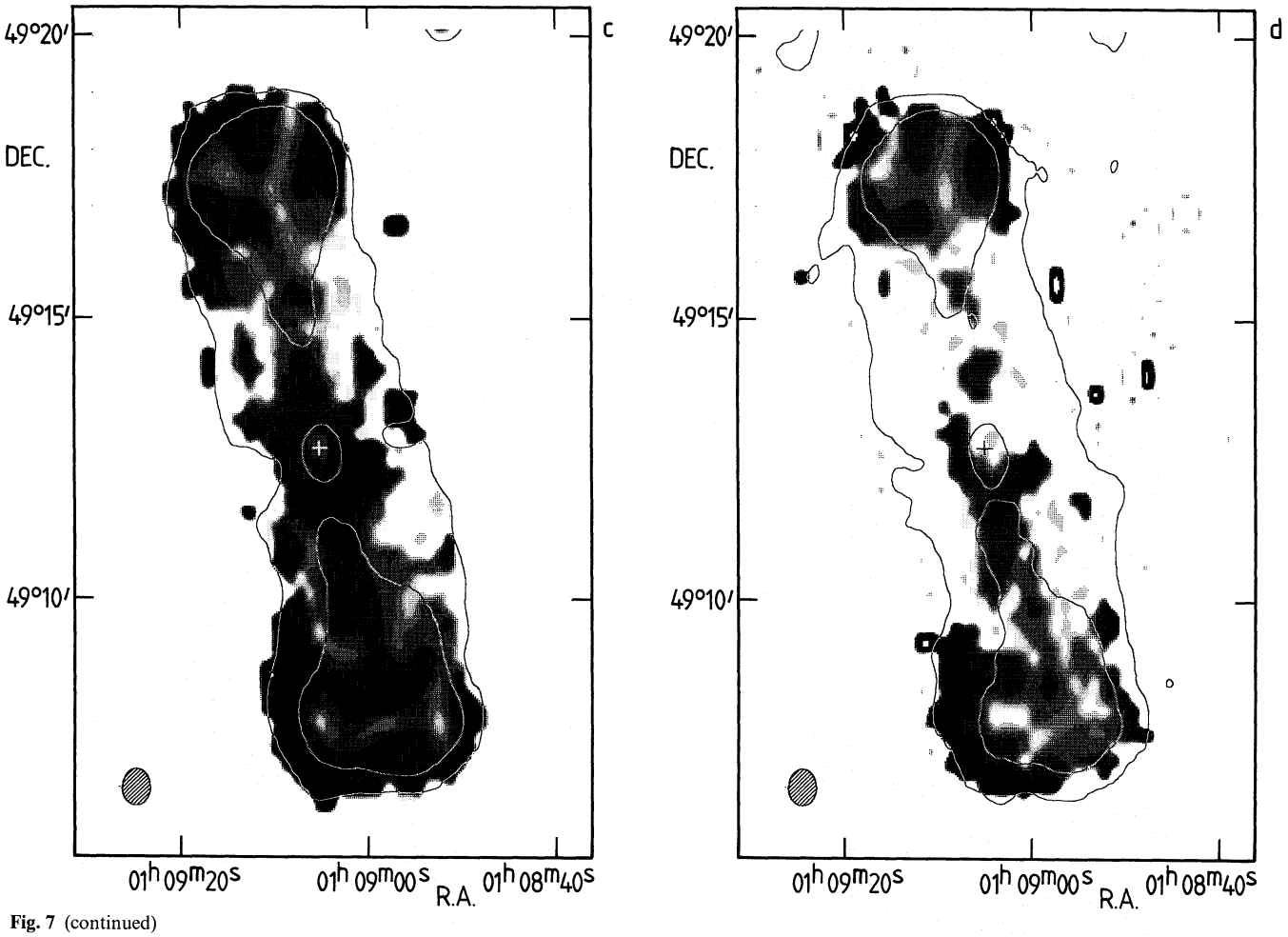

Fig. 7 (continued)

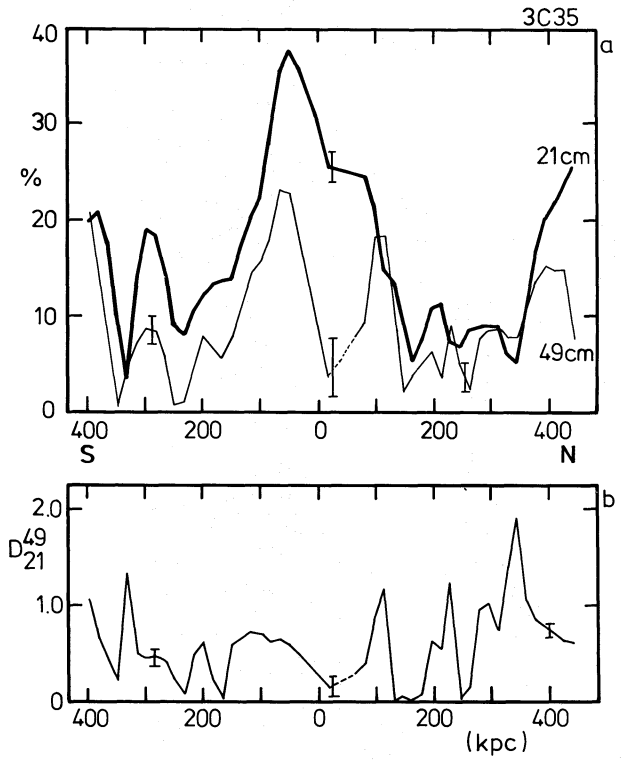

Fig. 8a and b. Crosscuts along the major axis of 3C 35 for **a** the degree of polarization at the two wavelengths and **b** the depolarization ratio D_{21}^{49}. Dashed lines indicate upper limits to the values, and error bars give typical uncertainties where they are much greater than the line thickness. The optical galaxy coincides with the origin of the abscissa

In Fig. 11 the electron density is shown as a function of distance from the galaxy nucleus for each of the X-ray haloes (one density value determined at r_c for each object) and for several locations along the lobes of the two radio galaxies. A power-law relationship of the form $n \propto \text{distance}^{-m}$ provides an excellent fit to all data points (coefficient of determination $= -0.98$) for $m = 1.58$, and this is shown as a solid line.

The X-ray brightness distributions also provide information on the density profiles of individual galaxies, although as Thomas et al. (1986) note, the slopes of these profiles are "poorly determined" because of uncertainties in the background count rate. By using the density determined at r_c for each galaxy such uncertainties are minimized. Figure 11 demonstrates that the X-ray haloes for these early-type galaxies are all quite similar. Forman et al. (1985) note that for an isothermal gas, their adopted surface brightness distribution leads to a density profile of the form $[1+(r/r_c)^2]^{-3\beta/2}$. For the typical value of β obtained from their fits to the X-ray data ($\beta = 0.5$) the outer parts of the density profiles should decline as $r^{-1.5}$, close to the value found above. The precise relationship ($n \propto [1+(r/r_c)^2]^{-3/4}$) is shown by a dashed line for one of the galaxies (NGC 1316), and it is seen to provide a satisfactory fit to both the X-ray and radio data points. While the density profiles derived from the radio polarization data are not as steep as $r^{-1.5}$, the limited angular resolution will cause an overestimate of P at 49 cm for small r (where the gradient in n is steep), and hence an underestimate of n. We must now consider what sort of behavior is expected before we can decide whether the radio derived gas densities are indeed the outer parts of X-ray haloes.

Let us derive the expected relationship for the simplest possible case, making the following assumptions:

– Hot gas is trapped in the gravitational potential well of a massive galaxy;

– The mass of gas is small enough, at least in the outer regions we are interested in, that it does not perturb the gravitational potential well. Justification for this can be found in the rough mass estimate from depolarization data made above (several times $10^9 M_\odot$) which is much less than the mass of a giant elliptical galaxy;

– There are no bulk motions, the hot gas being in hydrostatic equilibrium.

From this last condition, we have (e.g. Gull and Northover, 1975):

$$\frac{dp}{dr} = -\varrho G \frac{M_0}{r^2}, \tag{3}$$

where p is the pressure of gas with density ϱ at a distance r from the center of the mass concentration, M_0, responsible for the gravitational potential. Further assuming $p\varrho^{-\gamma} = \text{const} \equiv p_0 \varrho_0^{-\gamma}$, where γ is the polytropic index of the gas, we have:

$$dp = \gamma \varrho^{\gamma-1} p_0 \varrho_0^{-\gamma} d\varrho = -\varrho G \frac{M_0}{r^2} dr. \tag{4}$$

Which gives by integration:

$$\varrho^{\gamma-1} \frac{\gamma}{\gamma-1} = \frac{\varrho_0^\gamma}{p_0} \left(G \frac{M_0}{r} + \frac{\Pi_\infty}{P_\infty} \right), \tag{5}$$

where Π_∞ / P_∞ is a constant of integration with the units of pressure/mass density. Rearranging Eq. (5), we obtain

$$\varrho = \varrho_0 \left[\frac{\gamma-1}{\gamma} \frac{\varrho_0}{p_0} \left(G \frac{M_0}{r} + \frac{\Pi_\infty}{P_\infty} \right) \right]^{1/(\gamma-1)}. \tag{6a}$$

If we take

$$\frac{\Pi_\infty}{P_\infty} \equiv \left(\frac{\varrho_\infty}{\varrho_0} \right)^{\gamma-1} \frac{\gamma}{\gamma-1} \frac{p_0}{\varrho_0}$$

then we see from substitution in Eq. (6a) that $\varrho = \varrho_\infty$ at a large distance from the galaxy. As discussed by Gull and Northover (1975) if the galaxy is immersed in a general gaseous background ($\varrho_\infty \neq 0$) its gravitational potential will merely perturb the ambient gas density. For simplicity we will consider the case $\varrho_\infty = 0$ ($\Pi_\infty / P_\infty = 0$), so Eq. (6a) becomes:

$$\varrho = \varrho_0 \left(\frac{\gamma-1}{\gamma} \frac{\varrho_0}{p_0} G \frac{M_0}{r} \right)^{1/(\gamma-1)}. \tag{6b}$$

Assuming $\varrho(r_0) = \varrho_0$, then

$$r_0 = \frac{\gamma-1}{\gamma} \frac{\varrho_0}{p_0} G M_0. \tag{7}$$

For a well-stirred, adiabatic gas such as that found in clusters of galaxies (e.g. Gull and Northover, 1975), $\gamma = 5/3$. Typical values for the gas parameters at $r_0 = 10$ kpc obtained from the X-ray measurements are $p_0 = 2\ 10^{-12}$ erg cm^{-3} and $n_0 = 10^{-3}$ cm^{-3}. These can be inserted in Eq. (7) to estimate the mass producing the gravitational potential, M_0: $M_0 = 2\ 10^{12} M_\odot$, not an unexpected value for a giant elliptical galaxy and very similar to what was found by Forman et al. (1985). From Eq. (6b) with $\gamma = 5/3$, we have

$$n = n_0 (r_0/r)^{1.5}. \tag{8}$$

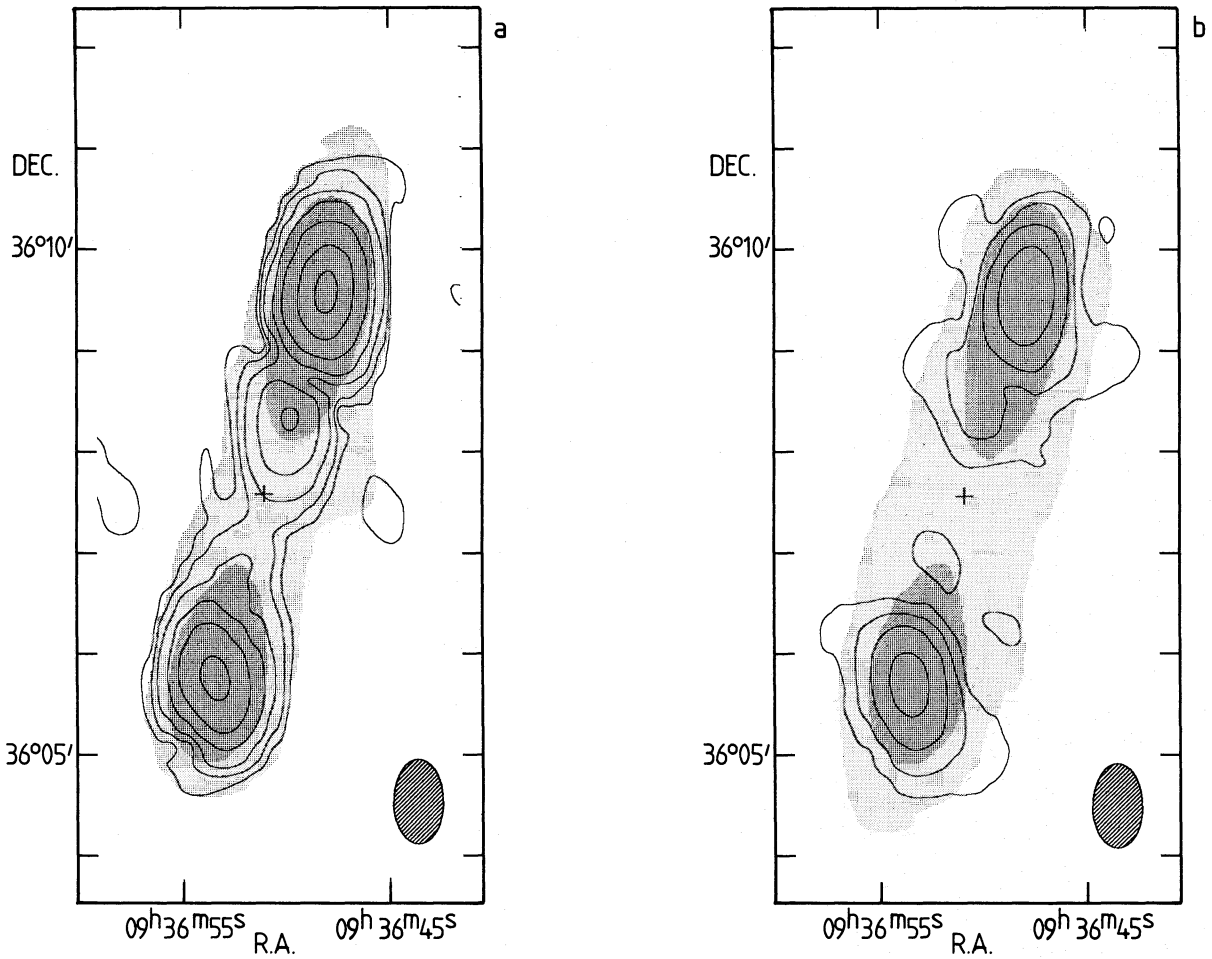

Fig. 9a–d. The polarization distribution in 3C 223. The polarized intensity P is shown as contours superimposed upon the total intensity brightness distribution I in gray at **a** 21 cm (contour values: 2.5, 5, 10, 20, 40, 80, and 120 mJy beam^{-1}) and at **b** 49 cm (contour values: 15, 30, 60, and 120 mJy beam^{-1}). The degree of polarization is shown as gray shading with contours from the total intensity at **c** 21 cm and **d** 49 cm. The lightest shade of gray indicates a value below 2%. Thereafter, the degree of polarization increases logarithmically to 20% (black). A cross indicates the position of the optical galaxy

This agrees well with the best fitting power law. Indeed, since some of the values for r_c are upper limits (Table 2 and Fig. 11), we might expect the observed power law relationship to be slightly less steep. If we exclude the upper limits, the best fit gives $n \propto r^{-1.54}$. An alternative approach to assuming $\gamma = 5/3$ is to use the best-fitting parameter to solve for γ: from Eq. (6b) we then have, $(\gamma-1)^{-1} = 1.54$, which gives $\gamma = 1.65$.

The data are, thus, in excellent agreement with what would be expected from a halo of ionized gas gravitationally bound to each central galaxy and extending out to radii of at least 100 kpc. In view of the assumptions made in our calculation the haloes should be spherically symmetric, although the radio data have enabled us to sample the gas distributions along only two radii per galaxy. We can integrate Eq. (6b) to calculate the mass of gas in the halo beyond r_0:

$$M_{\rm gas} = \int_{r_0}^{r} \varrho \, dV = 4\pi \varrho_0 r_0^{1/(\gamma-1)} \int_{r_0}^{r} r^{(2\gamma-3)/(\gamma-1)} \, dr \,. \tag{9}$$

We then obtain for the total mass of the outer part of the halo (exterior to r_0)

$$M_{\rm gas} = 4\pi \varrho_0 r_0^3 \, \frac{\gamma-1}{3\gamma-4} \left[\left(\frac{r}{r_0} \right)^{(3\gamma-4)/(\gamma-1)} - 1 \right]. \tag{10a}$$

The mass thus increases with the size of the halo.

For the parameter values assumed above, we have

$$M_{\rm gas} = 2\ 10^8 \left[\left(\frac{r}{10\,\rm kpc} \right)^{3/2} - 1 \right] M_\odot \,. \tag{10b}$$

Consequently, we can see that $M_{\rm gas}$ will only approach M_0 for $r > 4$ Mpc, while the mass between 10 kpc and 100 kpc will be $6\ 10^9\ M_\odot$. Only if the haloes should be shown to extend much beyond 1 Mpc would the possibility exist that they might contribute significantly to the galaxy mass.

5. Conclusions

The observations presented and discussed in this paper, together with X-ray measurements, strongly suggest that extensive haloes gravitationally bound to early-type galaxies are a major cause of depolarization in double radio sources as was surmised by Strom and Conway (1985). This is probably also the dominant factor in the depolarization-size correlation found and discussed by Strom (1973a): He observed excess depolarization at 49 and 73 cm in sources whose components were less than about 60 kpc from the optical identification. Since that correlation was based upon measurements of the integrated polarization in double sources,

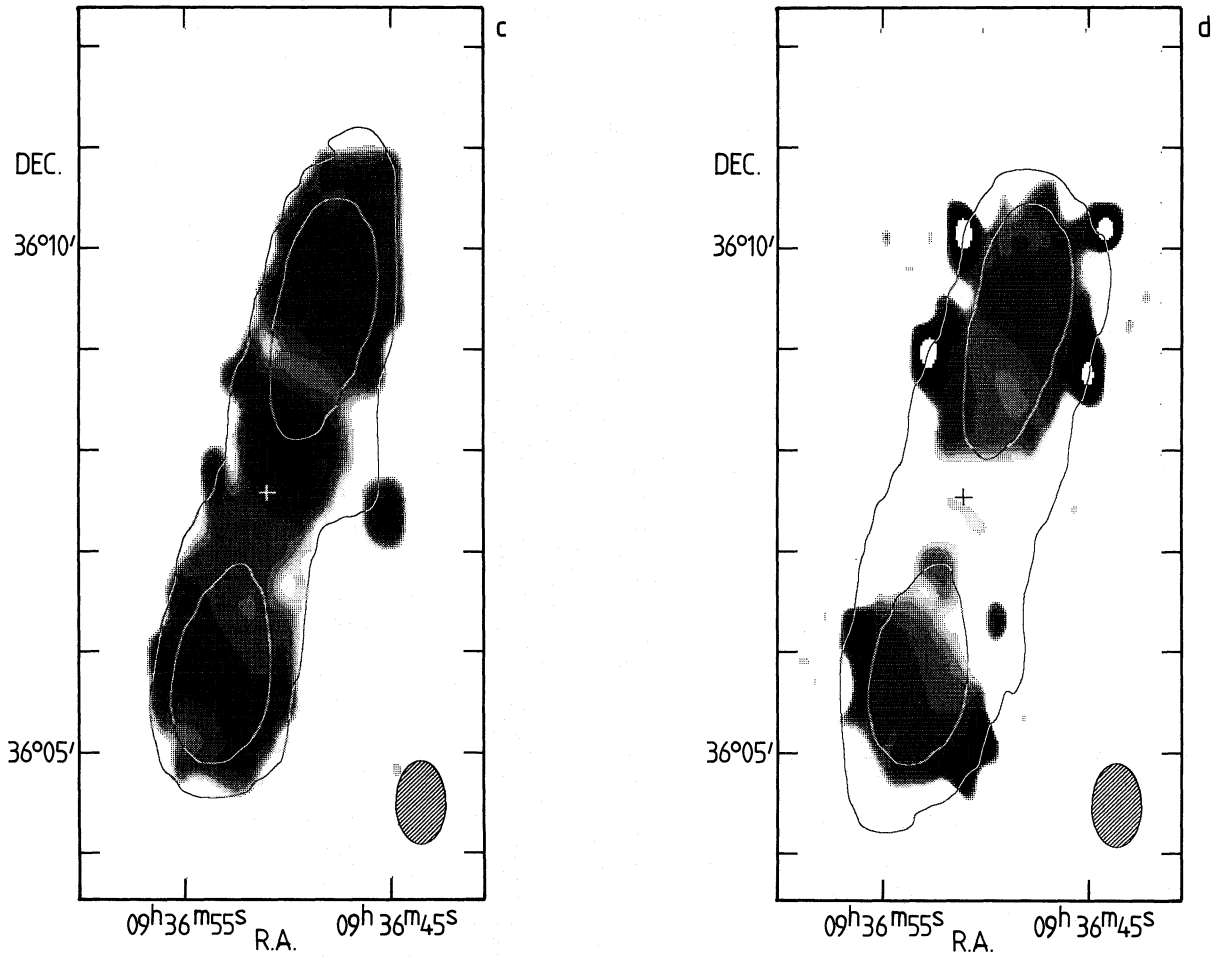

Fig. 9 (continued)

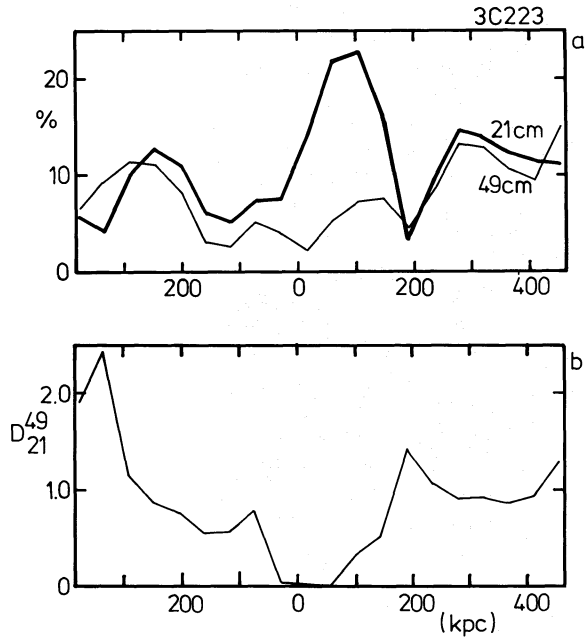

Fig. 10a and b. Crosscuts along the major axis of 3C 223 for **a** the degree of polarization at the two wavelengths and **b** the depolarization ratio D_{21}^{49}. The optical galaxy coincides with the origin of the abscissa

Table 2. Parameters of X-ray haloes around early-type galaxies

Galaxy	Type	r_c (kpc)	$n_{th}(r_c)$ (10^{-3} cm^{-3})
NGC 315	E/SO	$\leqq$5.4	6.4
NGC 1316	SO	1.4	12.6
NGC 1332	E/SO	$\leqq$2.8	5.3
NGC 1395	E2	$\leqq$6.5	2.6
NGC 2563	SO	$\leqq$8.8	2.3
NGC 3607	SO	6	1.3
NGC 4374	E1	2.0	12.7
NGC 4382	SO pec	$\leqq$4.0	2.3
NGC 4406	E3	3	8.4
NGC 4472	E2	1.5	19.9
NGC 4594	Sa	$\leqq$9.3	2.6
NGC 4636	E0	1.6	18.2
NGC 4649	E2	$\leqq$2.0	19.9
NGC 5846	E0	2.6	23.8

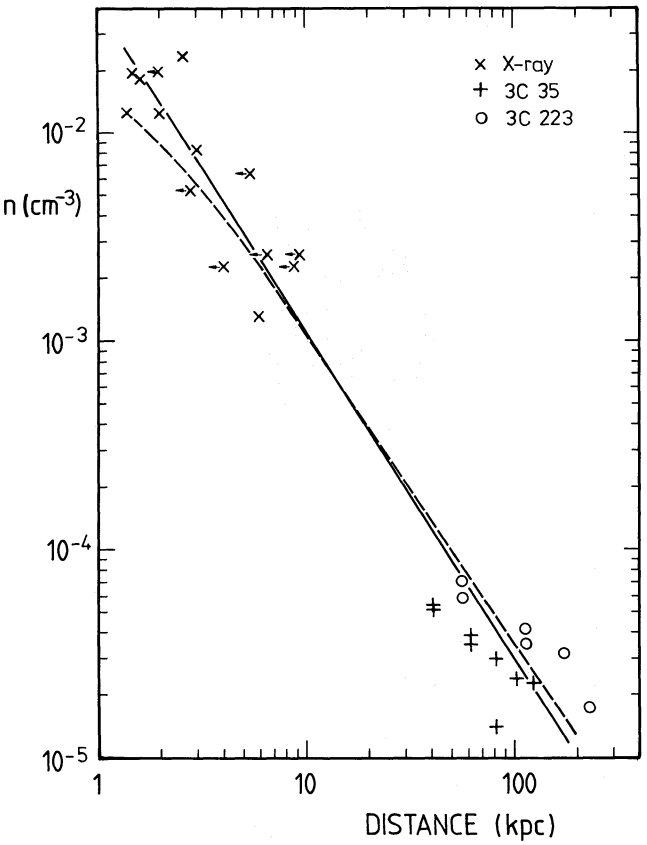

Fig. 11. The thermal density as a function of distance from the nucleus derived from X-ray observations for 14 early-type galaxies (Table 2) and from radio depolarization for two double radio galaxies. Arrows indicate data points for which the r_c value may be an upper limit. The solid line is a least squares fit through the data of the form $n \propto r^{-m}$ where $m = 1.58$ gives the best fit. The dashed curve shows the expected variation in $n(\propto [1-(r/r_c)^2]^{-3/4})$ for $r > r_c$.

it could not have been surmised, as we have demonstrated here, that the central bridge emission (a relatively insignificant component) in large doubles is depolarized at 49 cm. The fact that all doubles smaller than about 120 kpc display excess depolarization is further evidence for the ubiquity of extensive haloes associated with early-type galaxies. Moreover, Strom's correlations show that such haloes probably surround quasars as well.

X-ray emission from the high-density inner regions of the halo shows that the gas is cooling. The gas causing radio depolarization in the outer halo lies beyond the typical cooling radius found from the X-ray data (Thomas et al., 1986); consequently it cannot cool within a Hubble time. The fact that the radial density variation (Fig. 11) is consistent with that expected for gas in hydrostatic equilibrium implies that its angular momentum is small. It is therefore possible that as the cooling gas from the inner halo condenses out, it will be replenished by slowly infalling material. Some of this, eventually reaching the nucleus, is a potential source of power for nuclear activity.

As was pointed out above, the amount of gas sampled by both the X-ray and radio polarization measurements amounts to no more than a percent or two of the galaxy mass. Thus the gas directly observed will not contribute significantly to any "dark" component which might be present. But the very fact that it conforms to the behavior expected of gas in hydrostatic equilibrium suggests that there is unlikely to be an additional component anyway: the gravitational field of any extra material would produce higher gas densities. Unless the continuity between X-ray and radio data exemplified by Fig. 11 is pure coincidence, the gaseous halo should be a good indicator of the gravitational potential, and it provides no evidence for "dark" matter beyond a radius of 10–40 kpc out to about 200 kpc. This may, however, contrast with the situation for dominant galaxies in rich clusters (e.g., Mathews, 1978).

It is clear that gas densities obtained from studies of radio depolarization at long wavelengths provide a useful complement to the higher densities implied by X-ray observations of haloes around elliptical galaxies. In this work we have only been able to make a detailed investigation of a handful of sources, so obviously investigations of more objects would be highly desirable. Moreover, such work should be carried out over a range of frequencies to enable $\lambda_{1/2}$, and hence the Faraday depth, to be determined in an unambiguous way. Short wavelength observations of the inner bridges would be valuable to see if depolarization produced by the high density X-ray cores can be detected. Such measurements would additionally provide an estimate of magnetic field strength against which the equipartition assumption can be checked, although the low surface brightnesses of radio bridges may be a serious limitation.

Longer wavelengths could be used to look for depolarization at distances much greater than 100 kpc from the parent galaxy, as we do not know how extensive the haloes actually are. However, as the measurements of 3C 35 show, there may be depolarization caused by other mechanisms (of unknown nature) present in the outer components, limiting the usefulness of the depolarization technique. On the basis of the existing data it seems unlikely that haloes will contribute more than 10% to the mass of a large elliptical galaxy. Even if they should extend as far as 1 Mpc, they will barely double the total estimated mass.

Finally, let us consider whether such extensive haloes might be detectable by other means – indeed, whether they might already have been observed. Sargent et al. (1980) in a study of Lyα absorption systems in distant quasars have argued that the absorption lines arise in intervening gas clouds at the cosmological distances indicated by their redshifts. The densities they obtain, $10^{-4} - 4\ 10^{-3}\,cm^{-3}$, and diameters for the clouds, 30 pc – 30 kpc, are similar to the halo parameters we find when account is taken of cosmological evolution. Typical column densities, N, range from 10^{16}–$10^{20}\,cm^{-2}$.

We can determine the column density along the line of sight at a projected distance x from the halo center by integrating Eq. (8) as shown in the appendix. From (A3) we get:

$$N(x) = 1.6\ 10^{20} \left(\frac{r_0}{x}\right)^{1/2} cm^{-2}, \qquad (11)$$

where the values found above for n_0 ($10^{-3}\,cm^{-3}$) and r_0 (10 kpc) have been assumed. Equation (11) shows that if the profile in Fig. 11 can be extrapolated to greater distances, then even for $x = 1$ Mpc or more, the column density will lie in the range found for the absorption-line systems.

There are, however, two possible objections to identifying the haloes we have been investigating with the distant clouds observed by Sargent et al. (1980). In the first place, Sargent et al. themselves conclude on the basis of a two-point correlation function analysis that the clouds are not distributed like galaxies and hence are unlikely to be associated with galaxy haloes. A second objection is the halo temperature, if the values found by Thomas et al. (1986) hold for haloes at large galactocentric distances and at high

redshifts. The temperatures derived by Sargent et al. are much lower than those suggested by the X-ray emission. The question clearly requires further investigation before a final conclusion can be drawn. The phenomenon may also be related to Lyα emission which has been detected in very distant galaxies (Djorgovski et al., 1985). In a recent investigation, McCarthy et al. (1987) found a 100 kpc "cloud" of Lyα emission which encompasses the radio source 3C 326.1 – its dimensions are thus similar to those of the depolarizing haloes we have been discussing.

Acknowledgements. RGS is grateful to Dr. P. Biermann for helpful comments and communicating unpublished data. He also wishes to thank Profs. J.H. Oort and R. Sancisi for reading and commenting upon the manuscript. The Westerbork Synthesis Radio Telescope is operated by the Netherlands Foundation for Radio Astronomy with the financial support of the Netherlands Organization for the Advancement of Pure Research (ZWO).

Appendix: integrating the halo volume density to obtain column density as a function of radius

The column density through the halo at a projected distance x from its center can be simply obtained by integrating Eq. (8):

$$N(x) = \int_{-\infty}^{\infty} n(x,y)\, dy = n_0 \int_{-\infty}^{\infty} \left(\frac{r_0}{(x^2+y^2)^{1/2}}\right)^{3/2} dy\,, \qquad \text{(A1)}$$

where $x^2+y^2=r^2$ and y is the position along the line of sight. Since $n(x,+y)=n(x,-y)$, we need only evaluate the definite integral $\int_0^{\infty} (x^2+y^2)^{-3/4}\, dy$, which appears in standard tables. This gives,

$$N(x)=2n_0 r_0^{3/2} \int_0^{\infty} (x^2+y^2)^{-3/4} dy = n_0 r_0^{3/2} x^{-1/2} \left[\frac{\Gamma(\frac{1}{2})\Gamma(\frac{1}{4})}{\Gamma(\frac{3}{4})}\right]. \qquad \text{(A2)}$$

The constant in brackets has the value 5.24, so there results

$$N(x) = 5.24\, n_0 r_0 \left(\frac{r_0}{x}\right)^{1/2} \mathrm{cm}^{-2}\,. \qquad \text{(A3)}$$

This result holds for that part of the halo where the density follows an $r^{-3/2}$ profile. Although it assumes that the halo extends to infinity, the contribution of the outermost parts to $N(x)$ is small.

References

Biermann, P., Kronberg, P.P.: 1983, *Astrophys. J.* **268**, L69
Biermann, P., Kronberg, P.P., Madore, B.F.: 1982, *Astrophys. J.* **256**, L37
Burn, B.J.: 1966, *Monthly Notices Roy. Astron. Soc.* **133**, 67
Conway, R.G., Birch, P., Davis, R.J., Jones, L.R., Kerr, A.J., Stannard, D.: *Monthly Notices Roy. Astron. Soc.* **202**, 813
Conway, R.G., Gilbert, J.A.: 1970, *Nature* **226**, 332
Conway, R.G., Gilbert, J.A., Kronberg, P.P., Strom, R.G.: 1972, *Monthly Notices Roy. Astron. Soc.* **157**, 443
Conway, R.G., Haves, P., Kronberg, P.P., Stannard, D., Vallée, J.P., Wardle, J.F.C.: 1974, *Monthly Notices Roy. Astron. Soc.* **168**, 137
Djorgovski, S., Spinrad, H., McCarthy, P., Strauss, M.A.: 1985, *Astrophys. J.* **299**, L1
De Vaucouleurs, G., de Vaucouleurs, A., Corwin, H.G.: 1976, Second Reference Catalog of Bright Galaxies, University of Texas Press, Austin
Feigelson, E.D., Berg, C.J.: 1983, *Astrophys. J.* **269**, 400
Feigelson, E.D., Schreier, E.J., Delvaille, J.P., Giacconi, R., Grindlay, J.E., Lightman, A.P.: 1981, *Astrophys. J.* **251**, 31
Forman, W., Jones, C., Tucker, W.: 1985, *Astrophys. J.* **293**, 102
Gardner, F.F., Whiteoak, J.B.: 1966, *Ann. Rev. Astron. Astrophys.* **4**, 245
Gull, S.F., Northover, K.J.E.: 1975, *Monthly Notices Roy. Astron. Soc.* **173**, 585
Jägers, W.J.: 1987, *Astron. Astrophys. Suppl. Ser.* **67**, 395
Mathews, W.G.: 1978, *Astrophys. J.* **219**, 413
McCarthy, P.J., Spinrad, H., Djorgovski, S., Strauss, M.A., Van Breugel, W., Liebert, J.: 1987, *Astrophys. J.* **319**, L39
Miller, L., Longair, M.S., Fabbiano, G., Trinchieri, G., Elvis, M.: 1985, *Monthly Notices Roy. Astron. Soc.* **215**, 799
Nulsen, P.E.J., Stewart, G.C., Fabian, A.C.: 1984, *Monthly Notices Roy. Astron. Soc.* **208**, 185
Rudnick, L., Jones, T.W., Fiedler, R.: 1986, *Astron. J.* **91**, 1011
Sargent, W.L.W., Young, P.J., Boksenberg, A., Tytler, D.: 1980, *Astrophys. J. Suppl.* **42**, 41
Strom, R.G.: 1973a, *Astron. Astrophys.* **25**, 303
Strom, R.G.: 1973b, *Nature Physical Science* **244**, 2
Strom, R.G., Conway, R.G.: 1985, *Astron. Astrophys. Suppl. Ser.* **61**, 547
Strom, R.G., Willis, A.G.: 1980, *Astron. Astrophys.* **85**, 36
Thomas, P.A., Fabian, A.C., Arnaud, K.A., Forman, W., Jones, C.: 1986, *Monthly Notices Roy. Astron. Soc.* **222**, 655
Van Breugel, W., Jägers, W.: 1982, *Astron. Astrophys. Suppl. Ser.* **49**, 529
Willis, A.G., Strom, R.G.: 1978, *Astron. Astrophys.* **62**, 375
Willis, A.G., Strom, R.G., Bridle, A.H., Fomalont, E.B.: 1981, *Astron. Astrophys.* **95**, 250